Vol. 05, No. 4 (2023) 709-720, doi: 10.24874/PES05.04.013

Proceedings on Engineering Sciences

www.pesjournal.net

INVESTIGATING THE DYNAMIC BEHAVIOUR OF A LINEAR VIBRATORY FEEDER

Cristiano Fragassa
Ana Pavlovic[1]
Luca Berardi
Giuliano Vitali

Received 23.01.2023.
Accepted 25.09.2023.
UDC – 622.647.7

Keywords:

Electromagnetic Vibrators, Resonance Test, Modal Analysis, Natural Frequencies

A B S T R A C T

A linear vibratory feeder is an instrument that uses vibration to "feed" material to a process or machine. It consists of a vibrating frame, an electromagnetic coil, a spring, and a tray or trough for conveying materials. The vibration causes the material to move along the tray or trough, ultimately moving the material to its desired destination. The motion analysis of different linear vibratory feeders was here performed and compared. Numerical modeling and experimental verification were combined in the way to investigate the dynamic response of vibratory feeders and their effect on feed particle accelerations on conveying. A close correspondence between the measured and predicted resonance frequencies was found. This information was conveniently used to improve machine designs.

1. INTRODUCTION

Vibrators have emerged as indispensable components across a myriad of industries globally, serving as a foundational technology that revolutionizes the orientation and selection of diverse parts. Their ubiquitous presence underscores their pivotal role in an array of processes spanning transportation, precise dosing, and meticulous packaging within multifaceted sectors such as pharmaceuticals, automotive, and food, among others. Irrespective of the specific technology employed, these systems universally adhere to a fundamental principle: the vibratory feeder serves as the driving force, instigating the movement of products by inducing vibrations along the feeder channel. As these vibrations permeate the channel, the individual pieces undergo a sequence of small, deliberate jumps, initiating a collective motion that propels the products forward with consistent and seamless efficiency.

The inherent mechanism wherein these pieces maneuver through a series of calculated jumps within the channel is the linchpin of their reliable and continuous movement. These nuanced movements coalesce harmoniously, orchestrating a rhythmic and synchronized progression, enabling the systematic transportation and manipulation of materials within the industrial processes.

The adaptability and versatility of vibrators in these operational processes underscore their significance in streamlining production, ensuring precision in dosing, and facilitating the seamless packaging of products across diverse industries. The vibratory technology's ability to precisely manipulate and propel components

[1] Corresponding author: Ana Pavlovic
E-mail: ana.pavlovic@unibo.it

or materials underpins its widespread integration, enhancing efficiency, minimizing errors, and optimizing throughput in a broad spectrum of industrial applications.

The use of controlled vibrations for generate movements does not represent a newfound technology, with the first scientific reviews dating back to the 60s, (as in Redford & Boothroyd, 1967 or Taniguchi et al., 1963), but its advancements in design and functional optimizations continue to be of significant interest today due to their enduring impact.

Two technical solutions are commonly used:

- **Pneumatic vibrators**: they generate vibration through the linear movement of a floating piston. Additional oscillating masses can be used to modify frequency and vibration force.
- **Electromagnetic vibrators:** they use the principle of electromagnetic induction to generate vibration. They consist of a coil of wire that is wrapped around a ferromagnetic core. When an alternating current flows through the coil, it generates a magnetic field that causes the core to vibrate.

Both solutions offer an excellent response to the common industrial need to move little objects (small mechanical parts, seeds, pills) allowing them to be kept separate.

This is also the reason why vibrators have been largely investigated in the years (as in Bzinkowski et al., 2022).

For instance, limiting the selection to applications strictly in line with the contents of the present work, in Kwong et al. (2015) conventional methods for cleaning and grading seeds commonly employed by companies in the seed industry are presented, including a special attention to the use of vibration. Seed cleaning and grading are essential processes for producing high-quality seeds.

The primary goal of seed cleaning is to remove unwanted materials such as plant debris, dirt, and other impurities from the seed. This is necessary to improve the germination rate, viability, and overall quality of the seed. Seed grading, on the other hand, involves sorting seeds into different classes based on their size, shape, and other physical characteristics.

But the utilization of vibrators does not only concern the seed industry. In Mircea et al. (2020) e.g., their application for separating contaminants from wheat seeds with benefit of food safety and production is described.

Finally, in Zhao et al. (2021), a review about the application of discrete element method in the research of agricultural machinery is available: this work can be considered a convenient basis on the use of numerical methods in predicting the effect of vibration on processes. For instance, regarding the simulation of cleaning processes,
Lenaerts et al. (2014) investigated the separation of straw and grain in the screening phase due to vibration by analysing the properties of straw and grains on screening speed. Li et al. (2011) and Wang et al. (2015) examined the influence of the operation parameters such as vibrational amplitude, frequency, and direction angle on screening time and efficiency. Han (2020) and Ma et al. (2015) optimized the structure of separation sieves to improve the screening process. Furthermore, using a CFD-DEM coupling method, the movement of particles in the air-screen cleaning was monitored by Li et al. (2011, 2012). Additionally, the centroid velocities of grains, stems, and light impurities in the air-and-screen cleaning process were studied by Xu et al. (2020), and their degree of dispersion was monitored to analyse the cleaning performance.

In Kannan et al. (2016) the separation process of heavy and light products (stones and grains, respectively) on a destoner deck was simulated. The research team then analysed the impact of variables such as deck inclination, vibration speed, and fluidizing air velocities on the segregation performance, and identified the optimal combination value that yielded the best results. Moreover, the following study, by Kannan et al. (2017) aimed to improve by numerical methods the efficiency and accuracy of the destoning process, and the findings may have important implications for the agricultural industry. Additional relevant contributions are in Dučić et al. (2016) or in Ryba et al. (2022) about the use of advanced solutions in the design and calibration of vibratory feeders.

The present study was inspired by the objective to perfect an innovative dodder eliminator (‘decuscutor’) system, produced by *Millennium Green Srl*, Italy, able to quickly remove 100% of the dodder (i.e., 10 q. within 60 min.).

The dodder is a very resistant weed that must be totally eliminated in the production of seeds before their sowing. But this weed is tiny, difficult to select, thus specific techniques are needed, such as the use of iron powder and magnetic selectors: in the case, the transfer between these selectors is usually achieved by vibrators.
The machine under investigation is made up of two blocks (Figure 1): the first deals with mixing the seed with water, iron powder and oil with an exceptional method that uniforms the mix in an excellent way. The second block is formed by three rollers with permanent magnets, identical in shape but different from each other in terms of the content and quality of magnet of each one.

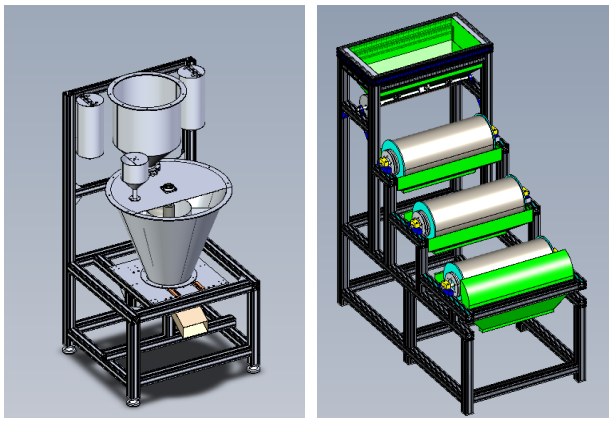

Figure 1. The first and second blocks of the dodder eliminator (‘decuscutor’)

Then, three pneumatic vibrators were used to drive three vibrating trays (Figure 2), which in turn conveyed the seeds towards the three permanent magnet rollers.

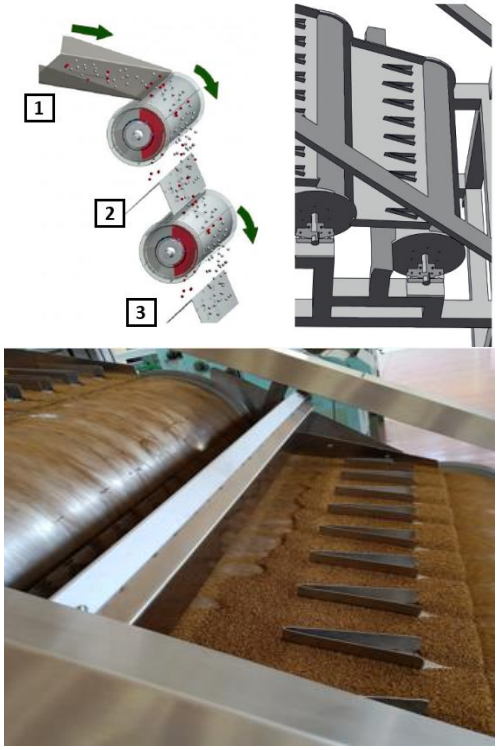

Figure 2. Seed sorting system made by vibrating trays and magnetic rollers.

This study aims to explore the possibility of replacing traditional pneumatic vibrators with electromagnetic vibrators, which offer several advantages such as simplified machine design, reduced weight and dimensions, and improved energy efficiency.
Outside the specific motivation, the analysis allowed us to investigate the dynamic behaviour of plates vibrated with electromagnetic vibrators by comparing simulations and experimental outputs. It was thus possible to understand, for example, how weights, materials, constraints, and loads can impact on the dynamic behaviour of structures and on their resonance conditions. An excellent connection between measurements and predictions emerged, as well as the evidence that minimal variations in the system conditions can modify, even markedly, the vibrational response of structures.

2. MATERIAL AND METHODS

2.1 Electromagnetic vibrators

An electromagnetic vibratory composed of a base unit, a coil, springs, a magnet, and a channel (Figure 3). The channel is connected to the base unit by the springs. The flat springs allow movement between the two, and it is this movement that will move the pieces. In simple terms, the coil (a ferrous core wrapped in copper wire to create an electromagnet) is attached to the base unit and the magnet is attached to the feeder channel. The coil attracts and releases the magnet, generating movement between the base unit and the feeding tray.

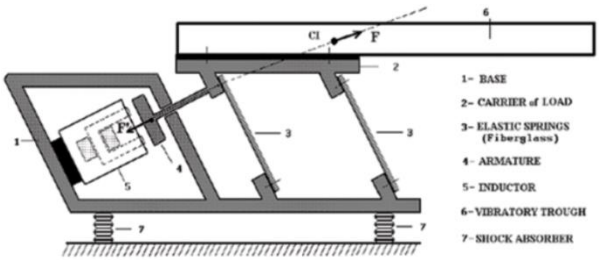

Figure 3. Diagram of a linear vibratory feeder (LVF)

The vibration of an electromagnetic feeder is generated when alternating electrical current moves back and forth through the wires of the coil. The magnet (attached to the feeder channel) is held a few millimetres from the coil by the springs. As the current moves in one direction, the coil attracts the magnet and adds tension to the springs. When the current changes direction, the magnet is released, and the potential energy stored as tension in the springs is used to vibrate the channel and advance the material. This active system, commonly named as vibratory feeder (conveyor) with an electromagnetic drive, is described in Ribic & Despotovic (2009) where useful considerations about its simulation and control (Tian, 2022) are also detailed.

Table 1. Main characteristics of trays under analysis.

Tray	Material	Dimensions (mm)	Thickness (mm)	Weight (kg)
A	**INOX**	399 x361x260	2.0	7.34
B	**STEEL**	964x501x205	2.0	10.25
C	**CFRP**	960x370x75	2.2	2.10

Specifically, a linear vibrator Mod. FT-01 by TARNOS was used, characterized by power, P = 20 W; current intensity, I = 0.4 A; weight, W =10 Kg; mass flow rate θ= $2 \cdot 10^3$ kg/h; maximum weight of feeder channel, W_f= 2.7 Kg; oscillation amplitude, a = 1.5 mm.

2.2 Vibratory tray

This study examined three trays that varied significantly in terms of shape, material, weight, and stiffness, while the thicknesses was approximately the same (2.0 ÷ 2.2 mm).

Specifically, as summarized in Table 1,

- **Tray A,** in stainless steel (Inox), thick and stick.
- **Tray B,** in carbon steel, thin, light, and cheap.
- **Tray C,** in carbon fiber reinforced plastic (CFRP), as flat laminate, ultralight and stiff.

The trays also differed in terms of technology readiness levels (TRLs): the first tray was already on the market, the second system was newly installed on a research machine, and the third tray was intended to demonstrate a proof-of-concept.

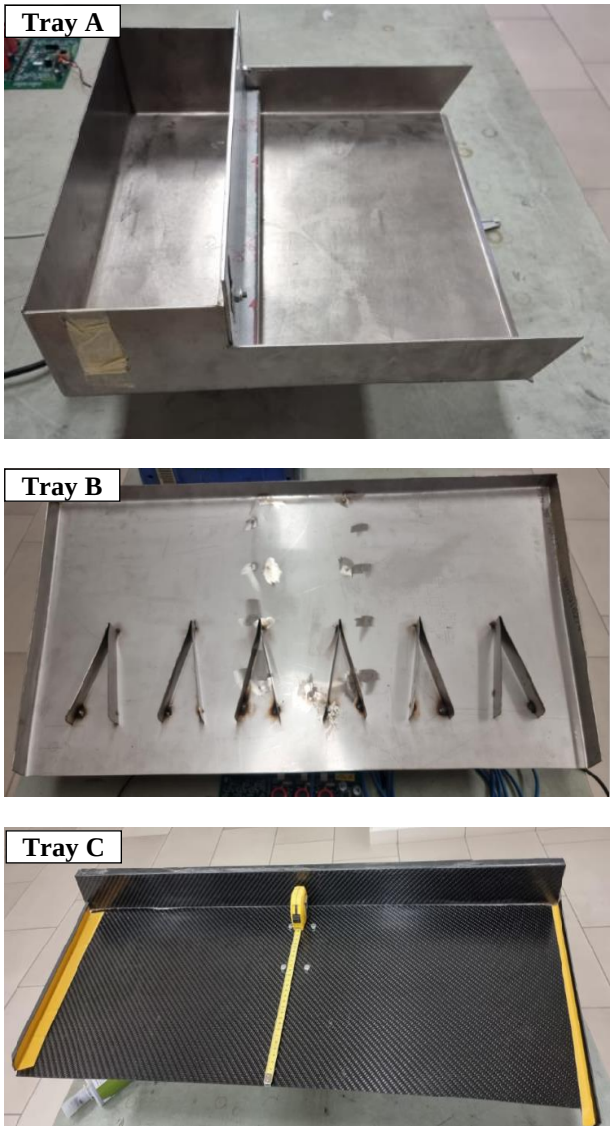

Figure 4. The three geometries under investigation

2.3 Mock-up

The experimentation took place by mounting each of the three trays (Figure 4) on the carrier of load (see component n. 2 in Figure 3). For the scope, support plates for fixing were designed and built. The trays use to be horizontally located (see component n. 6 in Figure 3). However, in the case of tray B, a 20° clockwise rotation was also tested, in the way to consider its original orientation inside the machine (Figure 2b). Examples of tray installation, at 0° (horizontally) and 20° on the linear vibratory feeder (LVF) are shown in Figure 5, for tray A and B, respectively.

Alfalfa (i.e., Medicago sativa L.) was used in the tests, a very common forage leguminous plant, with very small and light seeds (0.2 g / 100 seeds). The seeds were placed evenly on the upper band (~15cm) at the start of the trial (Figure 6). Their progressive redistribution over time was observed to obtain general indications on operation.

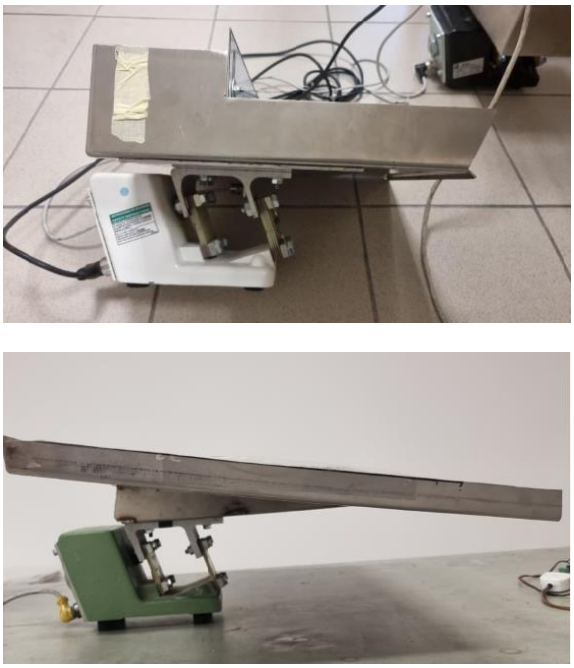

Figure 5. Trays mounted on the LVF

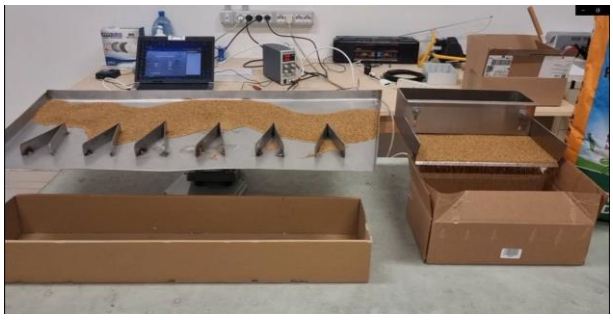

Figure 6. Experimental test example

In Figure 5, for instance, Tray A and Tray B are shown side by side (right and left, respectively) during a

parallel trial, permitted by the utilization of two vibrator feeders controlled by the same electronic controller. Both trays were loaded with a similar quantity of materials while the evolution over time was monitored.
An accelerometer, installed on the support (Figure 7), made it possible to measure the accelerations along the three axes depending on the excitation frequency. It was then possible to detect acceleration peaks and resonances.

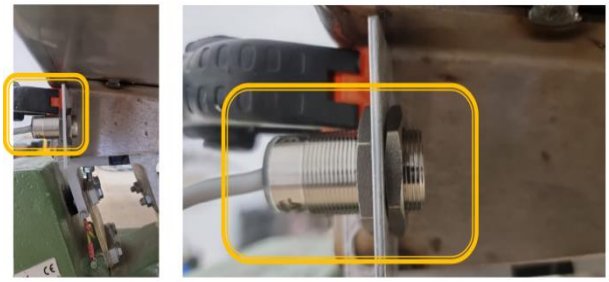

Figure 7. Accelerometer for measuring accelerations.

Specifically, the vibrator control system (*CV6Tool Ver 0.9.0.3*) is designed to operate in autotune, by modulating the excitation throughout the entire frequency range (up to 120 Hz) and then fixing the operation mode close to the resonance frequency. This process, allowed by feedback from the accelerometer, ensured high efficiency with low energy consumption.

2.4 Data availability

Data are provided on the control screen by two curves, as in Figure 8, both expressed respect to the time axis*(x)*: the acceleration and the frequency, labelled in the figure as *(a)* and *(b)*, respectively. They were measured and are here reported over the time: their values are expressed in the first and second y-axes, respectively, as a function of the time axis *(x)*. This also means that, with the scope to identify the frequency with respect to a given acceleration (e.g., a peak), it is necessary to combine the two curves. Practically, the path indicated by the dotted line in the case of 53 Hz (as example) must be followed.

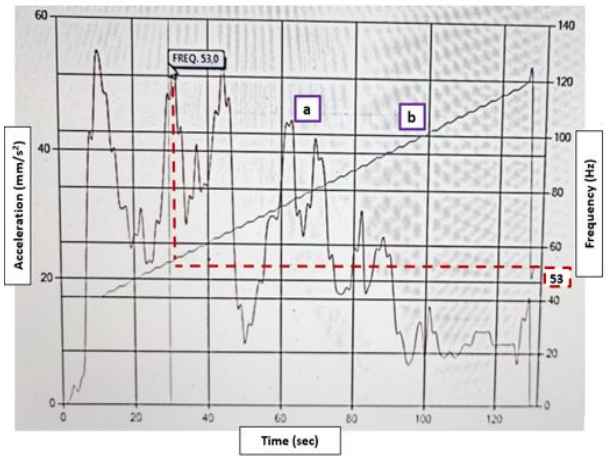

Figure 8. Data from measures

Phenomena of signal delays or hysteresis were also considered (as in Fragassa et al., 2016); however, it was verified that they were not relevant for results.

Finally, it should be remembered that acceleration represents the acceleration value measured at a specific point (where the accelerometer is rigidly fixed to the structure) and a specific direction (the one chosen as the direction to be monitored, usually the axial direction of the sensor). It also means that the self-calibration process of the system with respect to a specific frequency was done based on the acceleration measured (in a single point) with respect to a single direction.

These frequencies and results may differ when the frequency measurement direction is changed (this is an effect that was also investigated here). However, only the axis of advancement of material is of real interest due to its practical relevance.

Despite less complex than other experiments (as in Yazgi & Degirmencioglu, 2014 or Zhan et al., 2015), these measures turned out to be fit for purpose.

2.5 Simulation types

Simulations were performed by *Ansys Workbench Ver. 2023. With* the scope, previous similar studies were taken into account (such as Vujovic & Despotovic, 2015; Han & Gao (2010), Xu et al. (2017), Azhar & Shah, 2021; Han & Gao, 2010) including past deployments by the authors (Pavlovic, 2016 and 2017).

Two analyses were carried out:

- **modal analysis** to determine the natural frequencies, damping ratios, and mode shapes of a structure or system.
- **harmonic analysis** to investigate the dynamic behaviour for the system under vibration.

Both analyses were applied to investigate the systems' dynamic behaviour, but respect to different targets.

The modal analysis was used to validate finite element models, predict the resonances, identify structural weaknesses, optimize the structures' design. Its result was a set of natural frequencies (i.e., eigenfrequencies) and corresponding mode shapes of a structure or system. These frequencies and shapes represent the fundamental vibration modes of the structure or system and provide general information about its dynamic behaviour, such as its stiffness, mass distribution, and damping properties.

The harmonic analysis was used to study the system dynamic behaviour. Its result was a prediction of the system steady-state response to a periodic excitation (harmonic load) in the range of (40 ÷120 Hz). It provided information on the amplitude, phase, and frequency of the response, and could help identify

potential resonance or vibration issues. The analysis typically generated a frequency response plot that showed the magnitude and phase of the response as a function of frequency. Known results, also reported by authors in (Pavlovic, 2020), were used for the interpretation of the numerical results.

These distinct yet complementary analyses not only provided a comprehensive understanding of the systems' dynamic behavior but also laid the groundwork for informed decision-making. The modal analysis elucidated fundamental structural properties, whereas the harmonic analysis offered nuanced insights into the system's response under specific excitation conditions. By synergistically employing both methodologies, a holistic view of the system's dynamic behavior emerged, enabling a more refined optimization of structural designs and preemptive identification of potential vibration-related challenges."

2.6 System discretisation

In both analyses the same system discretisation was used.

- **Geometries** were modelled starting from trays' 3D shape. The following parts were also included: a) support plate, b) elastic elements, c) accelerometer, simplified as a metallic cylinder of similar dimensions.
- **Discretisation** was done by 3D finite elements (FEs) with rectangular or triangular base. Figure 9 shows, e.g., the discretisation of Tray A by 55442 solid elements and 186011 nodes.

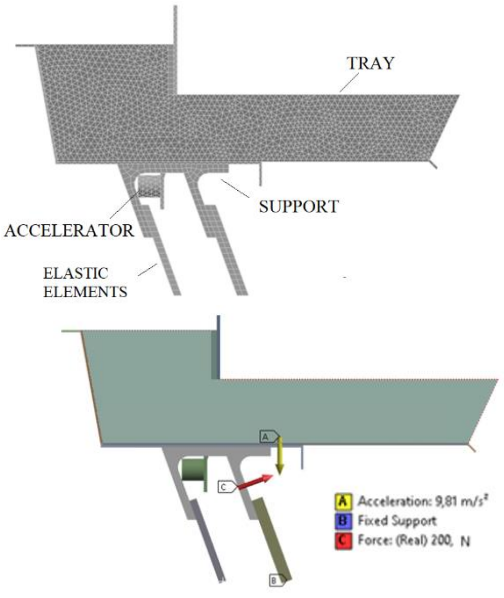

Figure 9. System discretisation (e.g., Tray A)

- **Conditions**, as external boundaries, and loads were applied to the harmonic analysis only. The system was considered as constrained at the lower extremes (*points B*), subject to its weight (*arrow A*) and to an impulsive force of 200 N (*arrow C*). This intensity was estimated starting from the technical characteristics of the device. The force was oriented orthogonally to the flexible elements, i.e., at 20° to the horizontal.
- **Material properties** considered how the trays were made of, namely Inox 304, C40 and *TorayT700*®(bidirectional) CFRP. The S-Ply®, a glass fibre reinforced polymer (GFRP) for leaf springs was used for the two elastic elements.

The characteristic properties of such materials, as density (ρ), elastic modulus (E), Poisson coefficient (ν), tensile strength (σ), and elongation at break (ε), are available in Table 2.

Table 2. Main material properties (isotropic).

Property	Material	AISI Inox 304	Steel C40	CFRP T700®	GFRP S-Ply®
ρ	g/cm^3	7.9	7.85	1.41	2.60
E	GPa	200	200	61	8.8
ν	--	0.3	0.3	0.28	028
σ	MPa	460	650	805	780
ε	%	45	18	1.2	4.5

However, given the orthotropic behaviour of reinforced composites (CFRP and GFRP), their parts were modelled using the Ansys ACP module, with particular emphasis placed on the orientation of the fibres. Their orthotropic properties were derived from other similar investigations (i.e., De Paola et al., 2013 and Fragassa et al., 2020 for CFRP and Vujovic & Despotovic, 2015 for GFRP) and are visible in Table 3. Together with the directional elastic modulus (E, GPa) respect to the *x, y, z* directions, the Poisson coefficient (ν) and shear modulus (μ , GPa) on *xy, yz, xz* planes are reported.

Table 3. CFRP and GFRP orthotropic properties

Property		CFRP	GFRP
E_x, E_y, E_z	GPa	61, 61, 6.9	8.8, 8.8, 0.37
ν_{xy} , ν_{yz}, ν_{xy}	--	0.04,0.3,0.3	0.28, 0.28,0.28
μ_{xy} , μ_{yz}, μ_{xy}	GPa	3.2, 2.7, 2.7	0.75, 3.3, 3.3

3. RESULTS AND DISCUSSION

3.1. Experimental measures

The experimental measurements of acceleration, *a(t)* and frequency, *f(t)*, both detected as function of the time (*t*) as exemplified in Figure 8, were combined to derive the relation between acceleration and frequency, *a(f)*,i.e., the *frequency response curve*. This curve shows how the system's acceleration varies with the frequency of the harmonic excitation and it was discretized by 40 points. Results are shown in Figure 10 (in the case of acceleration along the *x-axis*) for tray A and B.

It was immediately evident how the two systems present similar trends, with a significant acceleration peak, around 55-58 Hz (which is the expected LVF operational setup) and some secondary peaks, much less relevant, around the values of 45, 76, 86 and 96 Hz.

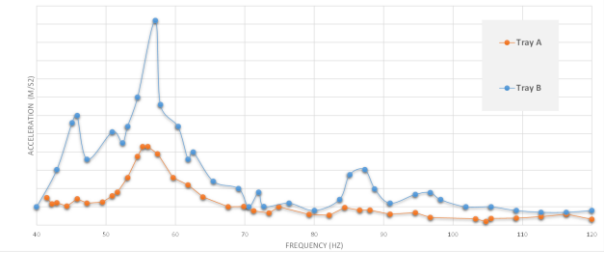

Figure 10. Experimental results: acceleration (*a*) vs frequency (*f*).

3.2. Modal analysis

The (numeric) modal analysis was performed in the range of≤120Hz, evaluating:

- **Eigen frequencies**, i.e., the frequencies at which the (three) systems vibrated freely without any external force applied to them. They were determined by the system's mass, stiffness, and damping properties. Table 4 lists the initial eigenvalues (≤ 120 Hz), as detected by the simulation, discarding the initial three, equal to zero, due to the fact they represented rigid body motions along the orthogonal axes. The first outcome was that the chosen LVF, operating at ≤120 Hz, appeared adequate to generate resonances in the systems. At the same time, these eigenvalues could not fit the experimental measures since the modal analysis, for how it operates, only considers a free body system.

Table 4. Natural frequencies (< 120Hz).

Tray	I	II	III	IV	V	VI	VII	VIII
A	12	15	113					
B	20	30	31	51	68	72	104	116
C	28	33	57	60	85	105	108	

- **Mode shapes**, i.e., the graphical representations of the deformation pattern of a vibrating structure at a given frequency (eigenfrequency). A mode shape was associated with every detected eigenfrequency. The deformation pattern of a mode shape was numerically determined combining the vibration amplitude and phase of each point on the structure. Figures 11-13 display such mode shapes depict the with areas of significant immobility highlighted in blue. The first two images in Figure 11, e.g., showed oscillations around the vertical (yaw) and transversal (roll) axes, respectively, while the 3rdimage looked like the superimposition of two distinct movements. Among these three mode shapes, the second one seemed to be the most appropriate for ensuring forward transport (along *x-axis*). Tray B and C exhibited 8 and 7 eigenvalues respectively, within the initial 120 Hz range, suggested a (significant) lower stiffness compared to tray A. This is also confirmed by the mode shapes: deformation patterns, typical of a slender structure, showed them inappropriate for the intended application.

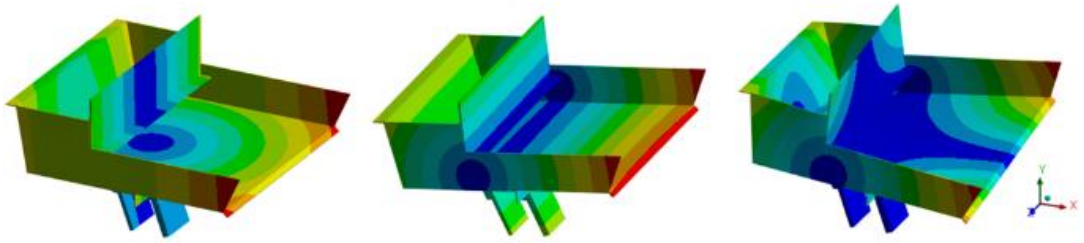

Figure 11. Mode shapes in the case of tray A (at 12, 15, 113 Hz).

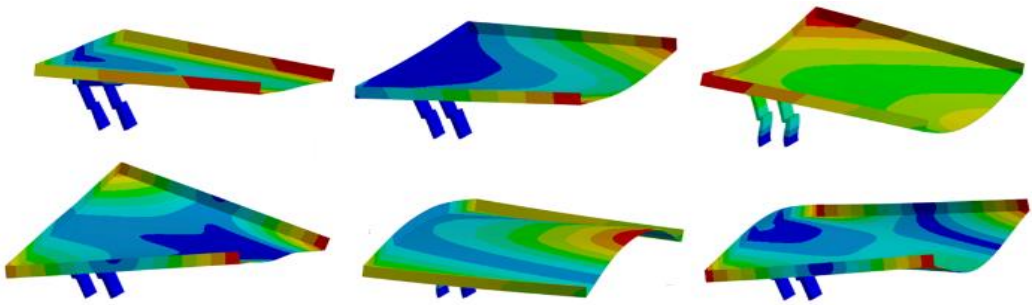

Figure 12. Mode shapes in the case of tray B (at 20, 30, 31, 51, 68 and72Hz).

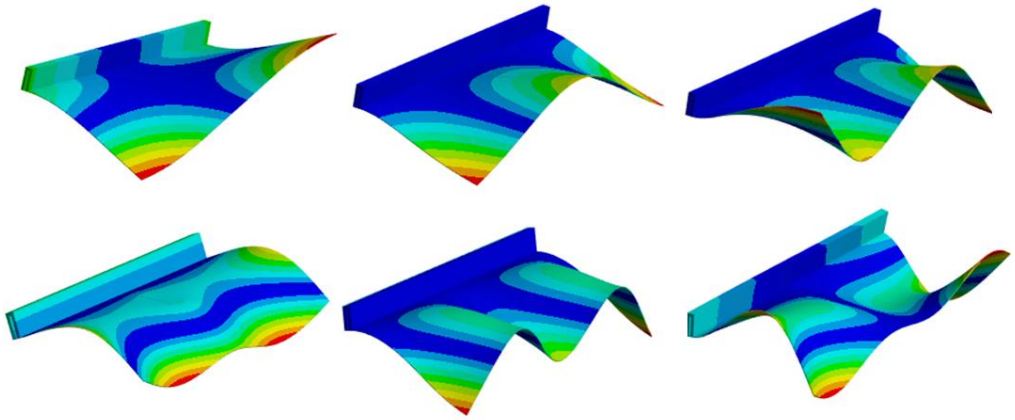

Figure 13. Mode shapes in the case of tray C (at 28, 33, 57, 60, 85 and 105Hz).

3.3. Harmonic response

The (numeric) harmonic analysis was performed in the range of 40 -120Hz, evaluating:

- **frequency response curve,** i.e., the relationship between acceleration and frequency, which depicts how a system responds to harmonic excitation across a range of frequencies. This curve, one per each tray, was compared with the one obtained experimentally with the scope to assess the ability of the FE model to predict the experimental results. Such an acceleration was estimated at the position of the accelerometer and respect to *x*-axis (as more representative). This comparison, shown in Table 5 and Figure 14, pointed out an excellent correspondence with the highest resonance correctly predicted each time (gapΔ<5 *Hz*, error $\Delta_{\%}$~5-7%) despite the uncertainty of materials' properties taken from literature. Moreover, the simulations emphasized further frequencies for resonances, some of which also emerged from the experimental data. The main difference, however, consisted in the numerical tendency of exalting the resonance phenomena predicting them more relevant than they were proved. This was probably due to the lack of dumping effects inside the numerical model.

Table 5.. Resonance frequency (Hz).

	Exp.	Sim.	Δ	$\Delta_{\%}$
Tray A	52	55	3	-5.5%
Tray B	51	55	4	-7.3%
Tray C	62	--	--	--

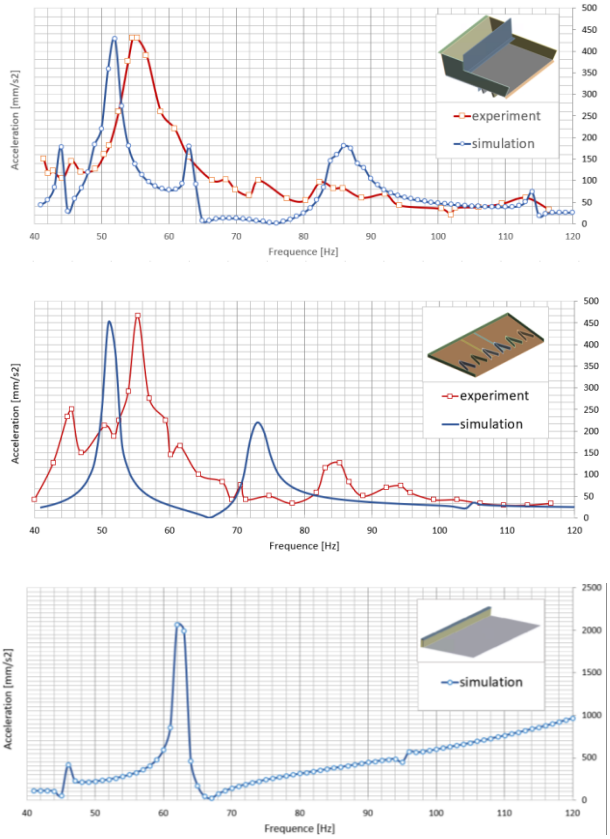

Figure 14. Frequency response curve

Limiting to the resonance frequency (i.e., 55 Hz), the harmonic response also permitted to identify:

- **displacements**, i.e., the displacement of each point, given as the contribution of the rigid body displacement and the structural deformation. This information was accessible respect to the cyclic load evolution. In Figure 15, e.g., the total and directional displacements in the case of Tray A are shown for to 55 Hz. The vertical deformation was much higher than the others (28.2 vs 4.1 and 5.2 mm).

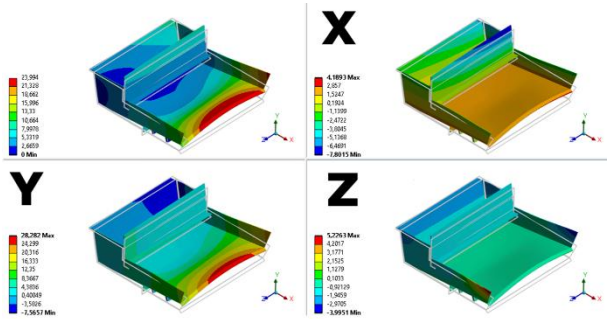

Figure 15. Total and directional deformations (case tray A, at 55 Hz)

- **stress/strain state,** which, however always remained under the yield stress of the materials, as was to be expected (<50MPa), as in Figure 16. These systems may encounter issues related to fatigue, corrosion, and fretting, but are not typically prone to failure resulting from exceeding operating loads.

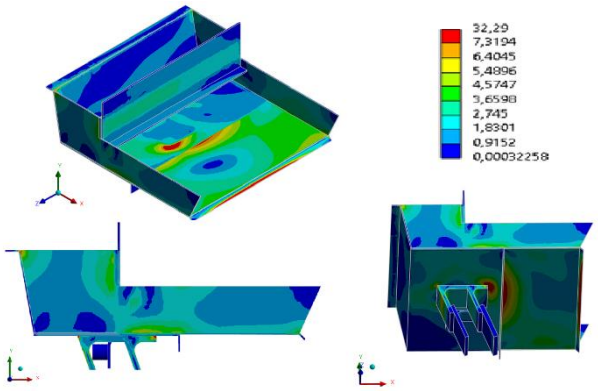

Figure 16. Equivalent stress (case tray A, at 55 Hz)

- **transport dynamics** was also investigated. The movements of materials (e.g., seeds) along the conveyor under vibration is rather complex, with additional aspects to be considered (e.g., physical and material properties of seeds as in Zhan et al., 2015). However, preliminary information is available thanks to the present investigation. In Figure 17, in the case of Tray C, for instance, it is possible to recognize the correspondence between the areas in which the seeds remained massed and those in which a displacement close to zero was estimated.

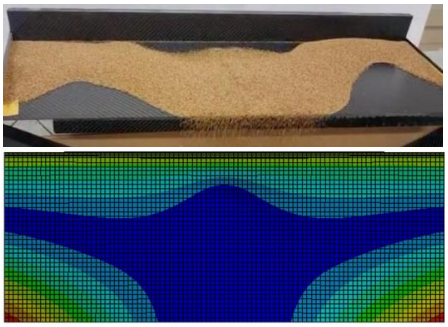

Figure 17. Transport dynamics (case tray C, at 62 Hz)

3.4. Further considerations

It is worth noting that the selection of the three trays for this study was based on their individual functionality.

- **Tray A** was continuously improved over time and it is now installed on different sorting lines (manufactured by IST Srl). Therefore, it served as a valid baseline for this analysis. At the same time, with a width half of what needed, design changes were necessary.
- **Tray B** was made considering the proper width and length since it was specifically designed to be installed on the new machine (by Millennium Green Srl) (Figure 2). At the same time, this tray was firstly designed to be used supported by an additional frame, which can no longer be considered as soon as LVFs will be introduced.
- **Tray C** intended to represent an alternative solution for stiffening the structure thanks to the use of carbon fiber reinforced plastic (CFRP). Characterized by a specific weight much lower than steel (1.6-3.5 vs 7.5-8.0kg/m^3), reinforced polymers are broadly used with the aim of improving stiffness-to-weight ratio. This benefit enhances when the CFRP material anisotropy is properly exploited, as well as different materials (e.g., honeycomb) are merged in layers. At the same time, due to the complexity behind the design and production of optimized composite sandwiches (i.e., use of molds and autoclaves), the experiment was limited to a CFRP laminate.

These preliminary considerations make it possible to better understand the proposed results and, in particular, the practical reason behind this study: with the analysis of Tray A, it was intended to develop and validate a numerical methodology able to support the redesign of Tray B, before moving on to the design of a new tray, based in structural terms on the material of Tray C.

4. CONCLUSION

A linear vibratory feeder, an instrumental apparatus harnessing vibrations for material delivery within industrial processes, operates as a multifaceted tool integrating several key components: a vibrating frame, an electromagnetic coil, a spring mechanism, and a conveyance structure—typically a tray or trough—dedicated to guiding materials. This ingenious system functions by imparting controlled vibrations to the materials, prompting their movement along the tray or trough, facilitating their seamless transportation to designated destinations within the process or machine.
In this comprehensive study, the focus was set on conducting a meticulous motion analysis, scrutinizing and comparing the performance of various trays integrated into a singular linear vibratory feeder. This

comparative analysis aimed to unravel the nuanced differences in their functionality and efficiency during material conveyance. Both numerical modeling and rigorous experimental verification were meticulously employed as a dual-pronged approach, aiming to dissect and comprehend the dynamic response of these vibratory feeders.

The analysis spanned the investigation of the effects induced on feed particles during the intricate process of conveying. Through a meticulous comparison between empirical observations and theoretical predictions, a compelling correlation emerged between the measured and predicted resonance frequencies. This alignment served as a critical validation of the theoretical models governing the behavior of vibratory feeders, offering invaluable insights into their operational dynamics.

The findings gleaned from this study not only validated existing theoretical frameworks but also paved the way for substantive improvements in machine designs. By leveraging the closely aligned resonance frequencies, engineers and designers gained invaluable insights to optimize and refine these vibratory feeders. These insights led to refined designs, bolstering the efficiency, precision, and reliability of these systems within industrial settings. The study's outcomes offered a critical stepping stone toward the advancement of vibratory feeder technology, ensuring enhanced performance and efficacy in material handling processes across diverse industries.

Acknowledgement: Special thanks to Francesco Gramenzi (Millennium Green S.r.l.) and Stefano Gnudi (I.S.T. S.r.l.) for their support to the investigation.

References:

Azhar, S., & Shah, S. I. A. (2021). Modeling and Analysis of a Vibratory Bowl Feeder. In *2021 Seventh International Conference on Aerospace Science and Engineering (ICASE)* (pp. 1-13). IEEE.

Bzinkowski, D., Ryba, T., Siemiatkowski, Z., & Rucki, M. (2022). Real-time monitoring of the rubber belt tension in an industrial conveyor. *Reports in Mechanical Engineering*, *3*(1), 1–10. doi:10.31181/rme200103002b

De Paola, S., Fragassa, C., Minak, G., & Pavlovic, A. (2013). Green Composites: a review of state of art. Carbon NY, 1, 230-240.

Dučić, N., Ćojbašić, Ž., Radiša, R., Slavković, R., & Milićević, I. (2016). CAD/CAM design and the genetic optimization of feeders for sand casting process. *Facta Universitatis, Series: Mechanical Engineering, 14*(2), 147-158. doi:10.22190/fume1602147d

Fragassa, C., Pavlovic, A., & Minak, G. (2020) On the Structural Behaviour of a CFRP Safety Cage in a Solar Powered Electric Vehicle. *Composite Structures 252*, 112698. doi: j.compstruct.2020.112698

Fragassa, C., Berardi, L., & Balsamini, G. (2016) Magnetorheological fluid devices: an advanced solution for an active control on the wood manufacturing process. *FME Transactions 44*(4), 333-339.

Han, L., & Gao, J. X. (2010). A Study on the modelling and simulation of part motion in vibratory feeding. *Applied Mechanics and Materials*, *34*, 2006-2010.

Han, M. (2020). Study on the Maize Threshing and Cleaning Mechanism with Low Loss and Anti-Blocking and Its Linkage Control. *Jiangsu University: Zhengjiang, China*.

Kannan, A. S., Jareteg, K., Lassen, N. C. K., Carstensen, J. M., Hansen, M. A. E., Dam, F., & Sasic, S. (2017). Design and performance optimization of gravity tables using a combined CFD-DEM framework. *Powder Technology*, *318*, 423-440.

Kannan, A. S., Lassen, N. C. K., Carstensen, J. M., Lund, J., & Sasic, S. (2016). Segregation phenomena in gravity separators: A combined numerical and experimental study. *Powder Technology*, *301*, 679-693.

Kwong, F. Y., Sellman, R. L., Jalink, H., &Schoor, R. V. D. (2005). Flower seed cleaning and grading. In *Flower seeds: biology and technology* (pp. 225-247). Wallingford UK: Cabi Publishing.

Lenaerts, B., Aertsen, T., Tijskens, E., Ketelaere, B., Ramon, H., Baerdemaeker, J., & Saeys, W. (2014). Simulation of grain-straw separation by a discrete element approach with bendable straw particles. *Computers and Electronics in Agriculture*, *101*, 24–33

Li, H., Li, Y., Gao, F., Zhao, Z., & Xu, L. (2012). CFD–DEM simulation of material motion in air-and-screen cleaning device. *Computers and Electronics in Agriculture*, *88*, 111-119.

Li, H., Li, Y., Tang, Z., Xu, L., & Zhao, Z. (2011). Numerical simulation and analysis of vibration screening based on EDEM. *Transactions of the Chinese Society of Agricultural Engineering*, *27*(5), 117-121.

Ma, Z, Li, Y. M., & Xu, L. Z. (2015). Discrete-element method simulation of agricultural particles' motion in variable-amplitude screen box. *Computers and Electronics in Agriculture*, *118*, 92–99.

Mircea, C., Nenciu, F., Voicu, Gh., Dumitru, I., & Oprescu, M. (2020). Review of the main equipment used for separating contaminants from wheat seeds, classification according to their functional role. *Annals of the University of Craiova-Agriculture, Montanology, Cadastre Series*, *50*(2), 380-385.

Pavlovic, A., Fragassa, C., Minak, G. (2017). Buckling Analysis of Telescopic Boom: Theoretical and Numerical Verification of Sliding Pads. *Tehnicki Vjesnik*, *24*(3), 729.735. Doi: 10.17559/TV-20160510143822.

Pavlovic, A., Fragassa, C., Ubertini, F., Martini, A. (2016). Modal analysis and stiffness optimization: the case of a tool machine for ceramic tile surface finishing. *Journal of the Serbian Society for Computational Mechanics*, *10*(2), 30-44.

Pavlovic, A., Sintoni, D., Fragassa, C., & Minak, G. (2020) Multi-Objective Design Optimization of the Reinforced Composite Roof in a Solar Vehicle. *Applied Sciences, 10*, 2665; doi:10.3390/app10082665

Pavlovic, A., Sintoni, D., Minak, G., & Fragassa, C. (2020) On the Modal Behaviour of Ultralight Composite Sandwich Automotive Panels. *Composite Structures*, *248*, no. 112523.

Redford, A. H., & Boothroyd, G. (1967). Vibratory Feeding. *Proceedings of the Institution of Mechanical Engineers*, *182*(1),135-152. doi:10.1243/PIME_PROC_1967_182_017_02.

Ribic, A. I., & Despotovic, Ž. V. (2009). High-performance feedback control of electromagnetic vibratory feeder. *IEEE Transactions on Industrial Electronics*, *57*(9), 3087-3094.

Ryba, T., Rucki, M., Siemiatkowski, Z., Bzinkowski, D., & Solecki, M. (2022). Design And Calibration Of The System Supervising Belt Tension And Wear In An Industrial Feeder. *Facta Universitatis, Series: Mechanical Engineering, 20*(1), 167-176. doi:10.22190/FUME201004026R

Taniguchi, O., Sakata, M., Suzuki, Y., & Osanai, Y. (1963). Studies on vibratory feeder. *Bulletin of the JSME*, *6*(21), 37–43.

Tian, Y. (2022). Frequency formula for a class of fractal vibration system. *Reports in Mechanical Engineering, 3*(1), 55–61. doi:10.31181/rme200103055y

Vujovic, M. M., & Despotovic, Ž. V. (2015, May). Dynamic stress distribution in composite leaf springs for electromagnetic vibratory feeder. In 3rd International Conference & Workshop Mechatronics in Practice and Education (MECHEDU) (pp. 14-16).

Wang, C. J., Liu, Q., Ma, L. Z., & Li, L. (2015).Cottonseed particle motion Law in 3-DOF hybrid vibration screen surface. *Transactions of the Chinese Society of Agricultural Engineering AgricultureEngineering*, *31*, 49–56.

Xu, L., Li, Y., Chai, X., Wang, G., Liang, Z., Li, Y., & Li, B. (2020). Numerical simulation of gas–solid two-phase flow to predict the cleaning performance of rice combine harvesters. *Biosystems Engineering*, *190*, 11-24.

Xu, Y. L., Wang, Q., Zhu, L. T., & Huang, D. Y. (2017). Numerical simulation and optimization for the vibration of the seed metering device based on a novel ML-IGA method. *Journal of Vibroengineering*, *19*(5), 3151-3168.

Yazgi, A., & Degirmencioglu, A. (2014). Measurement of seed spacing uniformity performance of a precision metering unit as function of the number of holes on vacuum plate. *Measurement*, *56*, 128-135.

Zhan, Z., Yafang, W., Jianjun, Y., & Zhong, T. (2015). Monitoring method of rice seeds mass in vibrating tray for vacuum-panel precision seeder. *Computers and Electronics in Agriculture*, *114*, 25-31.

Zhao, H., Huang, Y., Liu, Z., Liu, W., & Zheng, Z. (2021). Applications of discrete element method in the research of agricultural machinery: A review. *Agriculture*, *11*(5), 425.

Cristiano Fragassa
Department of Industrial Engineering,
University of Bologna
Bologna, Italy
cristiano.fragassa@unibo.it
ORCID 0000-0003-0046-8810

Ana Pavlovic
Department of Industrial Engineering,
University of Bologna
Bologna, Italy
ana.pavlovic@unibo.it
ORCID 0000-0003-2158-1820

Luca Berardi
AUTEC S.r.l.,
Fusignano (Ravenna),
Italy
berardi@autec-ra.it

Giuliano Vitali
Department of Agricultural and Food
Sciences, University of Bologna
Bologna, Italy
giuliano.vitali@unibo.it
ORCID 0000-0002-7866-5534